Hindawi Publishing Corporation
Science and Technology of Nuclear Installations
Volume 2007, Article ID 30863, 13 pages
doi:10.1155/2007/30863

Research Article

Atmospheric Transport Modeling with 3D Lagrangian Dispersion Codes Compared with SF6 Tracer Experiments at Regional Scale

François Van Dorpe, Bertrand Iooss, Vladimir Semenov, Olga Sorokovikova, Alexey Fokin, and Yves Margerit

Received 9 March 2007; Accepted 10 May 2007

Recommended by Giorgio Galassi

The results of four gas tracer experiments of atmospheric dispersion on a regional scale are used for the benchmarking of two atmospheric dispersion modeling codes, MINERVE-SPRAY (CEA), and NOSTRADAMUS (IBRAE). The main topic of this comparison is to estimate the Lagrangian code capability to predict the radionuclide atmospheric transfer on a large field, in the case of risk assessment of nuclear power plant for example. For the four experiments, the results of calculations show a rather good agreement between the two codes, and the order of magnitude of the concentrations measured on the soil is predicted. Simulation is best for sampling points located ten kilometers from the source, while we note a divergence for more distant points results (difference in concentrations by a factor 2 to 5). This divergence may be explained by the fact that, for these four experiments, only one weather station (near the point source) was used on a field of 10 000 km^2, generating the simulation of a uniform wind field throughout the calculation domain.

1. INTRODUCTION

In the case of risk assessment of nuclear power plant, the use of validated atmospheric transfer codes is essential to have an idea of nuclides ways of transfer in all compartments of the environment and properly estimate the impact of chronic or accidental atmospheric releases. Modeling the accidental release of radioactive or chemically toxic substances requires the development of atmospheric transport numerical model from a single concentrated emission source. The path of the resulting plume should be predicted, along with its arrival time at different locations. The ultimate goal is to obtain spatio-temporal maps of the products concentrations. Due to the financial and societal stakes, the simulations must have a high degree of accuracy because model predictions are often used for decision making strategies and environmental management. Various approaches and associated computer tools have been developed by different meteorological services, national protection agencies, or university laboratories (see, e.g., [1–4]). In order to improve these tools and promote their correct utilizations, the intercomparison between different models and associated results is an essential step [3, 5].

In this spirit and within the framework of a collaboration between the Commissariat à l'Energie Atomique (CEA, Cadarache, France) and the Nuclear Safety Institute of Russian Academy of Sciences (IBRAE, Moscow, Russia), this study presents some comparisons of 3D atmospheric transfer codes with field atmospheric tracer experiments. The principal goal is to challenge the code MINERVE-SPRAY, used by the CEA, and the code NOSTRADAMUS developed by IBRAE, with tracer experiments on a regional scale (several ten kilometers) with different weather conditions. Data used for the comparison come from four experiments which were carried out between 1983 and 1985 on a site in the North-East of Karlsruhe by the Kernforschungszentrum Institute of Karlsruhe (KfK) [6]. The main topic of this comparison is to estimate the Lagrangian code capability to predict the radionuclide atmospheric transfer on a large field. We wish also to reveal some potential limitations of the numerical models and some limits of our study.

The following section describes the two models that will be compared to a real experiment of tracer dispersion, which is presented in Section 3. Section 4 analyzes the numerical assumptions and differences between the two numerical models for the given experimental scenario. Results of the

intercomparison, based on statistical criteria classically used in previous studies, are presented in Section 5. A conclusion synthesizes our work.

2. DESCRIPTION OF 3D ATMOSPHERIC TRANSFER CODES

2.1. MINERVE-SPRAY code

The MINERVE code is a three-dimensional, regional scale, diagnostic meteorological model [7]. The model takes an arbitrary number of meteorological data (ground stations, profiles, large scale numerical weather prediction models output) and uses a detailed description of topography (digital terrain model, land use) to construct a sequence of refined 3D meteorological fields, including wind, temperature, and turbulence. Meteorological fields result from an optimal interpolation of the available data, under the constraints of mass conservation (continuity) and the control of vertical velocities by atmospheric stability (temperature gradients). The model also diagnoses the boundary layer evolution, computes turbulence using diagnostic formulations (O'Brien, Louis), producing both a turbulent diffusion coefficient K_z and turbulent kinetic energy. It runs in a terrain-following 3D coordinate system and is very fast (a few minutes for 24-hour simulations), thanks to the diagnostic approach which does not include complex time integrations. Its use is therefore recommended for emergency response purposes and for routine regular operation in forecast systems.

The SPRAY code is a three-dimensional Lagrangian dispersion model designed to simulate the dispersion of airborne pollutants, which takes into account spatial and temporal heterogeneities of both mean flow and turbulence [8, 9]. This code is based on a three-dimensional form of the Langevin equation flow [10, 11]. In the model based on Thomson's 1984 model, three-numerical schemes of different complexity are available to calculate the solutions of the equation system. In Thomson's 1987 model, more options are proposed in order to solve the equations such as schemes based on PDF of turbulent bi-gaussian velocities with different closures or Gram-Charlier series expansions. A detailed description of all the adopted schemes and associated equations can be found in [2].

SPRAY can be used with the wind field generated by MINERVE. The concentration fields generated from point, area, or volume sources can be easily simulated with this model. The behavior of the airborne pollutants is simulated using "virtual particles" whose mean movement is defined by the local winds and the dispersion is determined by velocities obtained as solution of Lagrangian stochastic differential equations, able to reproduce the statistical characteristics of the turbulent flow. Different portions of the emitted plumes can therefore experience different atmospheric conditions, allowing more realistic reproductions of complex phenomena (low wind speed conditions, strong temperature inversion, flow over topography, presence of terrain discontinuities such as land sea or urban rural), that are difficult to simulate with more traditional approaches like the Gaussian one.

2.2. NOSTRADAMUS code

NOSTRADAMUS is also a numerical code for prognosis of accident situations due to release of radioactive elements into the atmosphere. This code uses a Lagrangian trajectory stochastic model of atmospheric dispersion, a model of the atmospheric boundary layer for estimation of vertical profiles of meteorological parameters using surface observations, and a model for estimation of atmosphere stability class using synoptic information.

This stochastic model has some shortcomings. The ground-level concentration obtained with this method using a reasonable total number of particles (5 000–10 000) strongly fluctuates because of the lack of particles in the control volumes. To obtain smoother results, a modification of the Monte-Carlo method has been designed. In this modification every test particle is presented as a continuous cloud with a Gaussian concentration distribution. The concentration in a given location is now calculated as the sum of contributions from all the clouds. The cloud dimensions (horizontal and vertical radii) increase in time, so that the clouds may overlap during propagation.

To close the system of stochastic equations describing the propagation of pollutants in the atmosphere, it is necessary to determine the turbulent diffusion coefficients K_y and K_z as functions of location and the atmosphere conditions. The estimation of the vertical turbulent diffusion coefficient is described in [12]. The method is based on long-time observations at the meteorological tower of the "TYPHOON" institute (Obninsk, Russia), and takes into account similarity relationships for the atmospheric boundary layer. The boundary layer structure, given by the vertical profiles of diffusion coefficient $K_z(z)$, wind velocity $|V|(z)$, and direction $\theta(z)$, depends on the surface roughness, the mean wind velocity, and the stratification of the atmosphere (stability class). Typical profiles $K_z(z)$, $|V|(z)$, $\theta(z)$ for different stability classes are presented in [12].

NOSTRADAMUS contains an internal model for the atmospheric boundary layer (vertical distribution of wind velocity and turbulent diffusion coefficients) and a specific model for the evaluation of stability classes using synoptic data [13]. The coefficients used in these models are included in an internal database. The NOSTRADAMUS code does not take into account buoyancy effects. If a release is accompanied by thermal flux, the effective plume rise may be estimated using external stand-alone modules ("FIRE" [14] or "EXPLOSION" [14, 15]), or from an internal model based on Briggs' formulae [16]. It requires additional information that have to be provided by the user: thermal power; released gas temperature and density; released gas output velocity; and atmosphere temperature stratification (stability class).

3. EXPERIMENTAL INVESTIGATION

3.1. Site description

During the period 1983–1985, four mesoscale atmospheric dispersion experiments were performed near the

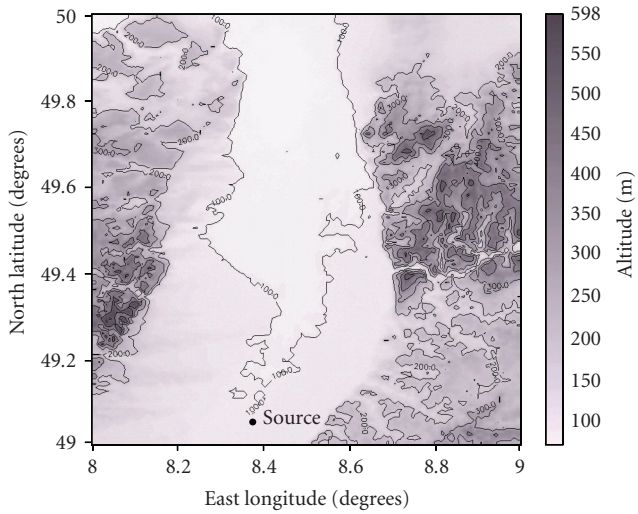

Figure 1: Topography of the domain and source locations.

Kernforschungszentrum Karlsruhe (KFK) [6]. The experiments were conducted as follows.

(i) Release of SF6 tracer gas at 100 to 140 meters height and downwind sampling at more than fifty locations during up to eight successive periods of 30-minute duration. Sampling was conducted at distances up to 60 kilometers from the source.
(ii) Meteorological measurements from a 200 meters height tower.

Figure 1 shows the topography of the domain and the source locations. The source is located about 50 kilometers northeast of Karlsruhe.

Measurements performed at the meteorological tower provide vertical profiles of temperature, wind velocity, wind direction, and standard deviation of vertical and horizontal wind direction. The frequency of data recording is 10 minutes. Readings were taken every 60 seconds to form the 10-minute averages and statistics. The wind direction was measured with a wind vane and the wind speed with a cup anemometer. The standard deviations of the horizontal and vertical wind directions were measured by means of vector vanes at 40, 100, and 160 meters height. The temperature gradient was calculated from the difference in air temperatures measured at 30 meters and 100 meters height.

3.2. *Tracer experiments*

All data described below are taken from [6]. The tracer was released from the stack after mixing with the air flow in the stack. The air was sampled at up to fifty locations downwind of the release point. The samplers were arranged along three concentric arcs (zones) surrounding the source, with minimum and maximum radii between 11 and 60 kilometers.

The tracer release rates of 22 to 29 g s^{-1} were estimated to be necessary for tracer detection above background level over all the sampling zones. The tracer emission rate was kept constant during all the experiments. All samplers inflated a plastic bag using a pump with a flow rate of 0.2 liter per minute. Several samples can be collected in sequential progression for fixed preselectable time periods. In all experiments, these periods were set to 30 minutes. Then all air samples were transported to the laboratory for chemical analyses. So measured values were the near-ground concentrations averaged over 30 minutes time interval.

For each experiment, the source location was the same (see Figure 1). The geographical coordinates of the source are 49.054 degrees north and longitude 8.3800 degrees east. All times are given in central European time (CET).

The characteristics of the four experiments are described in Table 1. Figure 2 shows the position of the sampling points for each experiment. For all experiments, the sampling points were organized into three arcs with different distances to the source (averaged distance), as shown in Table 2. Table 3 summarizes a part of the meteorological information during each experiment.

4. NUMERICAL ASSUMPTIONS

For the two numerical codes used, we used the same calculation assumptions for each experiment, as well as parameters physically representative of the environmental conditions and allowing to obtain computation results close to the near-ground measurements.

The domain considered for simulations is 100 kilometers by 100 kilometers as shown in Figure 1. The size of geographic cells is 0.890 km in the two geographic directions, and the height of the domain is 3000 meters (with twenty layers of progressive thickness: 10 meters for the first layer).

The assumptions and parameters used for the calculations are the following.

(i) Sufficiently broad field of simulation to avoid "boundary effects" of the field on the plume.
(ii) Constant value for the surface roughness over the entire domain: 1 meter.
(iii) Height of the of computation domain: 3000 meters; 10 meters thickness close to the surface, and 300 meters for the last cell, with a progressive thickness increase with altitude.
(iv) The classes of stability were considered as constant during each experiment which lasted only a few hours.
(v) In the two codes, the weather conditions were considered time dependent, according to the weather data record (record each 10 minutes).
(vi) The SF6 tracer was treated as a chemically inert gas, without deposition, with a density equal to that of the air, without washing of the plume (no rain during the four experiments) and without radioactive decay (tracer no radioactive).
(vii) The operational mode of tracer release was established for each experimentation according to the height of release, the emitted quantity, and the duration of the release.
(viii) The main difference between the two numerical codes is that MINERVE-SPRAY can take into account the

Table 1: Characteristics of the tracer experiments.

	Experiment 1	Experiment 2	Experiment 3	Experiment 4
Date	April 27, 1983	March 23, 1984	March 23, 1985	March 25, 1985
Tracer	SF6	SF6	SF6	SF6
Height of source (above ground level)	100 m	100 m	140 m	140 m
Release rate ($g\,s^{-1}$)	22.6	22.3	28.16	28.51
Duration of release	3 h 30 min	3 h	4 h 55 min	4 h 50 min
Release of tracer	10:00 am to 1:30 pm	11:00 am to 2:00 pm	11:00 am to 3:55 pm	10:30 am to 3:20 pm
Sampling of tracer	10:30 am to 3:00 pm	10:30 am to 3:30 pm	1:00 pm to 4:00 pm	1:00 pm to 3:30 pm
Number of monitoring points	21	32	48	50

effect of topography on the wind field. We did not note any significant effect of the topography for wind field results of the two codes.

(ix) In the case of MINERVE-SPRAY, the concentrations in SF6 were considered to be 10-meter height (at the top of the surface layer) whereas, during the experiments, the air sampling was carried out at 1 meter above ground.

A numerical limitation of MINERVE-SPRAY requires a surface layer higher than 10 meters in order to achieve numerical stability. Due to this fact, it underestimates the concentrations at this height. In the case of NOSTRADAMUS, the concentrations were computed at a 1 meter height for the comparison with the measurements at this height.

5. RESULTS

A comprehensive model evaluation methodology makes use of statistical evaluations using field data: model predictions are examined to see how well they match observations. In this section, we first illustrate some results of the numerical simulations. Then, we examine the results with a suite of different statistical performance measures.

5.1. Numerical results

Figures 3 to 6 show the calculated and observed SF6 concentrations along the three measurement arcs for the four experiments. Times were chosen to compare the results because the observations were reasonably complete at these times, as follows: 2 hours 30 minutes after the starting of the release for experiment 1 (Figure 3), 2 hours for experiment 2 (Figure 4), 3 hours 30 minutes for experiment 3 (Figure 5), and 3 hours for experiment 4 (Figure 6).

During the first experiment (Figure 3), the SPRAY code gives a good representation of the SF6 plume concentration for the first two arcs, and to a lesser extent with NOSTRADAMUS where the concentration is higher by a factor of 2 for arc 1. The calculated axis of the plume compares fairly well with the observed center. There are some differences in the evolution of concentrations particularly on arc 3, probably because of local meteorological conditions which are not identical to the global conditions used in the calculations.

For experiment 2 (Figure 4), we can point out the following results.

(i) On arcs 1 and 2, a fairly good agreement between measurements and calculations for NOSTRADAMUS and to a lesser extent for SPRAY.

(ii) for calculations with SPRAY, there is a difference by a factor of 4 to 5 (Arc 1) for the SF6 concentration compared to field measurements and NOSTRADAMUS results on the three arcs.

(iii) Possible errors in measurements at point 14 of arc 2 (missing concentration value), and probably at point 24 where the concentration is higher than that the value measured upstream on arc 2.

For experiment 3 (Figure 5), we can point out the following results.

(i) Difference of the plume axis between measurements and calculations, particularly on arcs 1 and 2 (variation from 1 to 2 kilometers between the measured and calculated axis).

(ii) The concentration levels are consistent with measured values for NOSTRADAMUS but lower by a factor of 2 with MINERVE-SPRAY.

And finally, for experiment 4 (Figure 6) we note the following.

(i) As in previous experiments, a fairly good agreement between measurements and calculations.

(ii) In this case, the axis of the simulated plume corresponds to measurements, but only on the first arc. On the two other arcs, we note a deviation of the plume axis (particularly for arc 2, with a deviation of a few kilometers) towards south east for the calculations compared with measurements.

For the four experiments, the SF6 concentrations calculated with MINERVE-SPRAY and NOSTRADAMUS are of the same order of magnitude as those measured near ground level. However, we can note some differences which are related to numerical assumptions. Note that the curves presented here are the instantaneous snapshots of the tracer plume during the calculations and the experiments. They do not represent the complete course of each measured and simulated data.

During the four experiments, we note a maximum variation of a factor 5 between the measured concentrations and those calculated (see experiment 2, Figure 4), showing

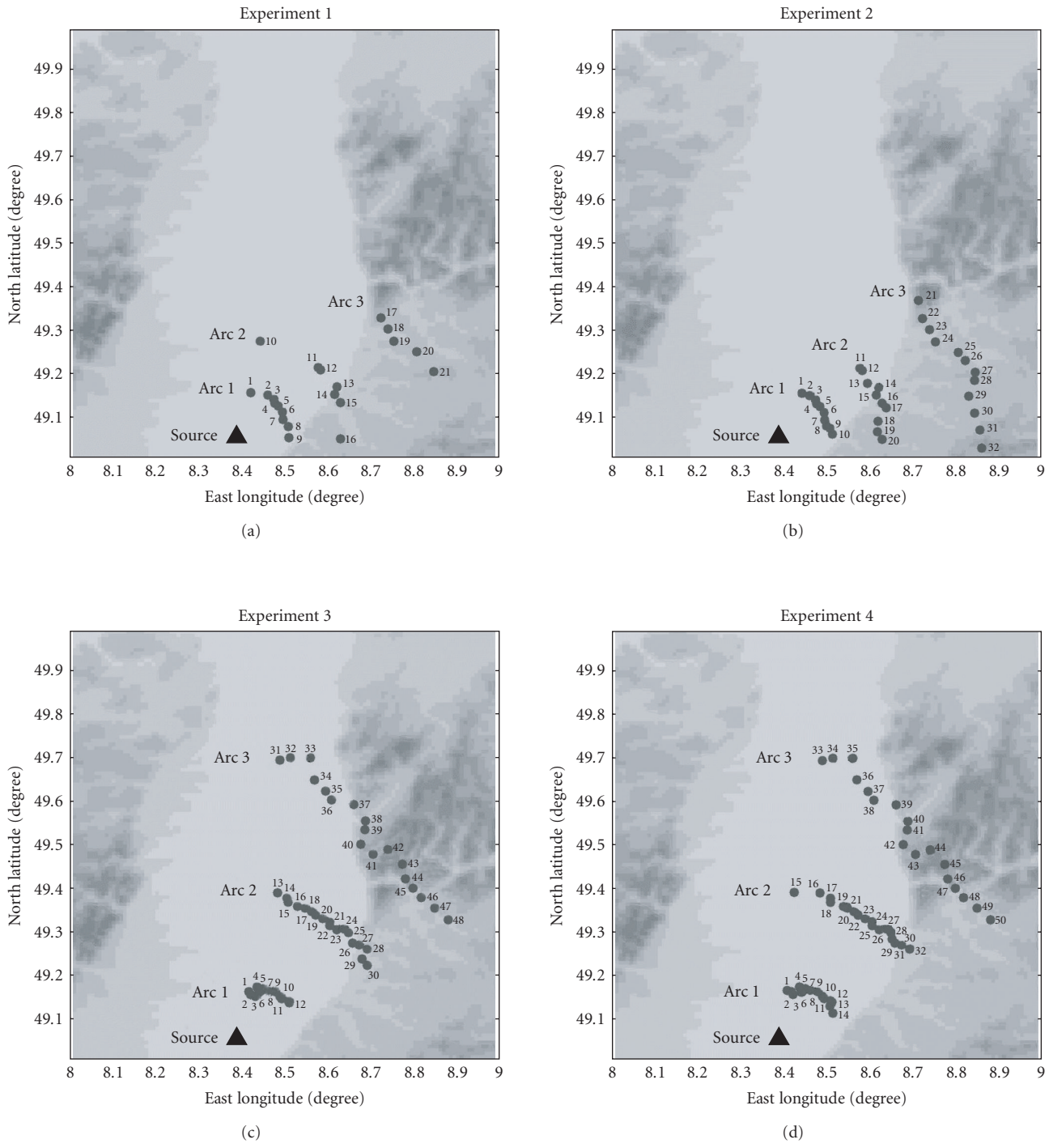

Figure 2: Positions of monitoring points for all experiments (topographic elevations in gray color scale).

Table 2: Positions of monitoring points for the four SF6 experiments.

	Arc 1	Arc 2	Arc 3
Experiment 1	11 km (points 1 to 9)	24 km (points 10 to 16)	42 km (points 17 to 21)
Experiment 2	11 km (points 1 to 10)	24 km (points 11 to 20)	45 km (points 21 to 32)
Experiment 3	12 km (points 1 to 12)	33 km (points 13 to 30)	60 km (points 31 to 48)
Experiment 4	12 km (points 1 to 14)	34 km (points 15 to 32)	60 km (points 33 to 50)

Table 3: Average weather conditions during the SF6 experiments.

	Wind direction at 40 m height	Average wind speed at 40 m height ($m\,s^{-1}$)	Atmospheric stability (Pasquill)	Average temperature at ground level
Exp. 1	Wind from SW (220 degrees +/− 20) with short variation in west direction (at 12:20 pm)	5.5	Classes B-C	14.8°C (max. variation of +7.2°C between 7:30 am and 2:20 pm)
Exp. 2	Wind from SW (220 degrees +/− 30), with a variation in west direction (between 1:10 pm to 3:30 pm)	6.0	Classes D-C	8.2°C (max. variation of −2.8°C between 8:30 am and 1:10 pm)
Exp. 3	Wind from SW (230 degrees +/− 40) with variation in south direction (3:10 pm to 4:40 pm and 6:00 pm to 7:40 pm)	4.6	Classes D-C	7.8°C (max. variation of −4.4°C between 9:00 am and 7:30 pm)
Exp. 4	Numerous variations of wind direction: wind of S, SW, E, SE, and *N* during this experiment	3.0	Classes C-B	11.3°C (max. variation of +8.3°C between 8:00 am and 4:30 pm)

the relatively good agreement between the codes and measurements. In general, MINERVE-SPRAY underestimates the concentrations because it considers the concentration at 10 meters above ground level instead of 1 meter (see design assumption). The axis of the plume is also fairly well represented by the codes with some notable differences, in particular during experiment 3 (a deviation of several kilometers on arc 1; see Figure 5).

A possible explanation for the discrepancy between calculations and experiments is that the simulated field has an important surface, 10 000 km^2 within a well-marked valley (see Figure 1) surrounded by hills of approximately 300 meters height, and the weather data are utilized only the tracer source location for each experiment. So, the three-dimensional wind fields are calculated with only one point of measurement and one obtains a uniform wind field, with a very weak terrain influence in the case of MINERVE-SPRAY. In the field, the reality is quite different, and the direction and speed of wind are not uniform across the site, in particular at 60 kilometers from the release point at the bottom of the hill. This may explain the differences in position of the axes of the plumes to short or long distance between measurements and simulations. In the case of MINERVE-SPRAY, a larger number of points would have improved the representativeness of the wind field.

5.2. Statistical analysis

It is important that a statistical model evaluation exercise should start with clear definitions of the evaluation objectives. In our study, the goals are to give some measures of the global accuracy of the numerical models, to indicate their potential limitations, and to detect the limits and problems of our study.

Different model evaluation methodologies and associated model performance measures have been recommended and developed for the air quality models [17, 18]. The authors of [5] have given a complete bibliography on this subject. Moreover, they recall the definitions and properties of the main important performance measures. In our analysis, we work in the framework of their definitions.

To statistically compare the results obtained by the codes with the field experiments, we utilize the bias and the mean square deviation. There are many other statistical criteria (sum of the absolute values, maximum, correlation coefficients, distribution of the residues, etc., see [5, 17]) but we note in this study that the bias and mean square deviation are more adapted and more interesting. Bias indicates if the numerical results are well centered on the experimental results, whereas the mean square deviation measures the discrepancy between calculations and measurements. The bias B is defined as the average of the differences between two sets X and Y of N data each:

$$B = \frac{1}{N}\sum_{i=1}^{N}(X_i - Y_i). \tag{1}$$

In our case, X data are the experimental results and Y data are the output given by the computer code (MINERVE-SPRAY or NOSTRADAMUS). We thus calculate the biases B(Spray) and B(Nostradamus). The mean square deviation (or mean square error) MSE is defined as the average of the squared differences between two sets X and Y of N data each:

$$\mathrm{MSE} = \frac{1}{N}\sum_{i=1}^{N}(X_i - Y_i)^2. \tag{2}$$

To compare the MSE with the bias value, we are interested in the square root of this value $\mathrm{RMS} = \sqrt{\mathrm{MSE}}$. We can thus calculate the values of RMS(Spray) and RMS(Nostradamus).

Table 4: Statistical criteria pairing in time and space.

	NOSTRADAMUS					SPRAY				
	NB	MG	NRMS	VG	FAC2	NB	MG	NRMS	VG	FAC2
Total	−0.01	0.34	2.58	15.6	0.17	0.5	0.58	2.97	36.1	0.13
Exp. 1	−0.87	0.25	2.55	27.8	0.14	−0.38	0.32	2.15	32.7	0.11
Exp. 2	−0.40	0.16	3.36	4.54	0.12	0.51	0.59	4.68	81.1	0.09
Exp. 3	0.47	0.39	2.69	12.7	0.21	0.90	0.61	3.19	54.5	0.16
Exp. 4	0.01	0.56	1.94	25.3	0.19	0.43	0.65	1.77	12.9	0.18

Table 5: Statistical criteria with the spatial averaging (by arc with time fixed).

	NOSTRADAMUS					SPRAY				
	NB	MG	NRMS	VG	FAC2	NB	MG	NRMS	VG	FAC2
Total	−0.26	0.80	1.33	5.29	0.35	0.25	1.31	1.50	4.84	0.38
Exp. 1	−0.81	0.71	1.43	1.61	0.52	−0.37	1.20	0.85	1.28	0.56
Exp. 2	−0.56	0.55	1.52	5.46	0.30	0.35	1.31	1.32	8.76	0.22
Exp. 3	0.17	0.94	1.05	7.96	0.28	0.56	1.39	1.50	10.1	0.39
Exp. 4	−0.25	1.26	1.33	13.9	0.20	0.21	1.10	1.07	4.34	0.33

Table 6: Statistical criteria with the temporal averaging (by time with spatial location fixed).

	NOSTRADAMUS					SPRAY				
	NB	MG	NRMS	VG	FAC2	NB	MG	NRMS	VG	FAC2
Total	0.06	0.70	1.62	7.74	0.35	0.55	1.11	1.96	13.2	0.25
Exp 1	−0.87	0.27	1.60	24.4	0.38	−0.38	0.39	1.31	83.2	0.14
Exp 2	−0.40	0.54	1.54	9.44	0.47	−0.51	1.24	1.73	12.7	0.28
Exp 3	0.47	0.89	1.90	4.03	0.33	0.90	1.32	2.44	14.5	0.27
Exp 4	0.01	0.94	1.17	7.44	0.28	0.43	1.32	1.05	5.67	0.26

To be able to compare biases and RMS in a rigorous manner, we normalize these values in the following way:

$$\mathrm{NB} = \frac{B}{\sqrt{\overline{X}\cdot\overline{Y}}}, \qquad \mathrm{NRMS} = \frac{\mathrm{RMS}}{\sqrt{\overline{X}\cdot\overline{Y}}}, \tag{3}$$

where $\overline{X}$ and $\overline{Y}$ are the arithmetic averages of X and Y. NB is called the normalized bias, and NRMS, the normalized root mean square error.

However, these two measures are known to be sensitive to large values and when the values vary by several orders of magnitude. Therefore, [5] propose to calculate two more robust criteria: the geometric mean bias

$$\mathrm{MG} = \exp(\overline{\ln X} - \overline{\ln Y}) = \frac{\underline{X}}{\underline{Y}}, \tag{4}$$

where $\underline{X}$ and $\underline{Y}$ are the geometric averages of X and Y, and the geometric variance

$$\mathrm{VG} = \exp\left[\overline{(\ln X - \ln Y)^2}\right]. \tag{5}$$

The authors of [5] also propose to use the fraction of data that satisfy $0.5 < X/Y < 2$, which is called FAC2. It is the most robust criterion because it is not sensitive to the distribution of the variables to be evaluated. Finally, in their paper, suggestions are given concerning the magnitudes of the performance measures expected of "good" models. It was concluded that a good model would be expected to have about 50% of the predictions within a factor of two of the observations (FAC2 > 0.5), a relative mean bias within [−30%, +30%] (|NB| < 0.3), and a relative scatter of about a factor of two or three (NRMS < 3).

In our study, the data are concentration values which depend on time, space, and experiment number (four experiments). The space coordinate is the distance between the source of the release and the three arcs of measurements where the concentrations are measured. To compare the results of the codes SPRAY and NOSTRADAMUS using the statistical criteria, several analyses are possible. The total analysis consists in taking all the values of concentrations obtained. We also analyze the data by distinguishing the experiments because their scenarios are different and results by experiment could be inhomogeneous. Moreover, three degrees of comparisons are made. Firstly, we perform the analysis by comparing each couple of concentrations defined by the same time and space (see Table 4). Secondly, as recommended by [17], we average the observations which are on the same arcs before the comparisons, and we compare spatial averages at a same time (see Table 5). This averaging process is often useful because slight changes in particle trajectories can lead to strong differences in calculated

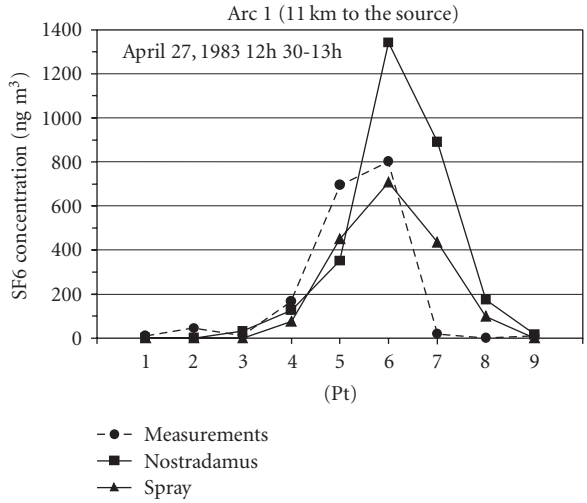

(a)

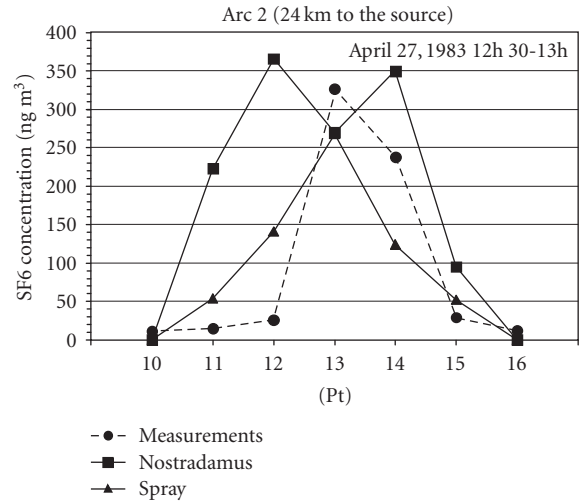

(b)

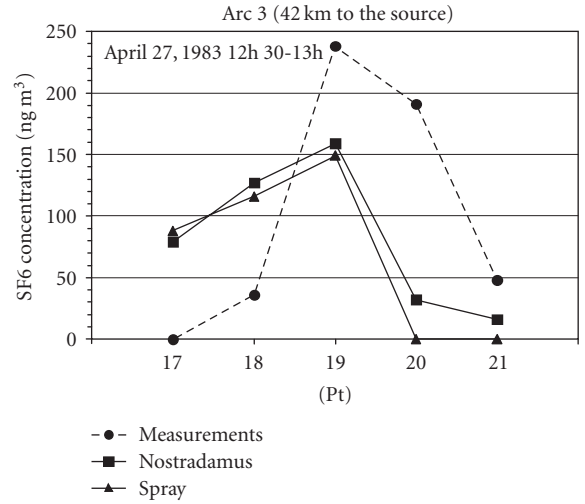

(c)

Figure 3: Comparison of SF6 concentration during experiment 1 on three arcs of monitoring points between measurements (at 1 meter above ground level) and NOSTRADAMUS and SPRAY calculations (at 10 meters above ground level).

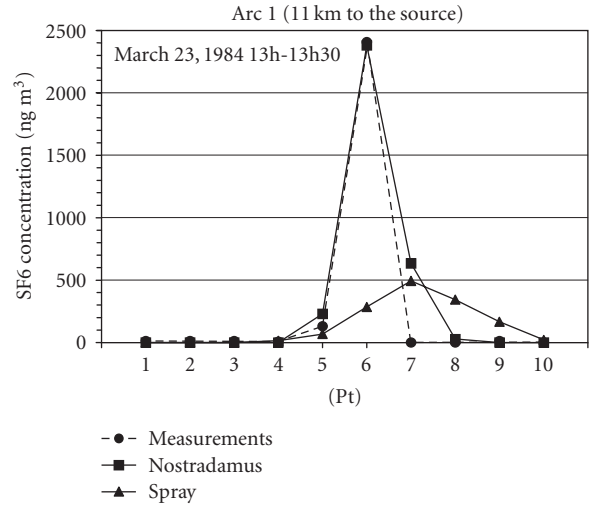

(a)

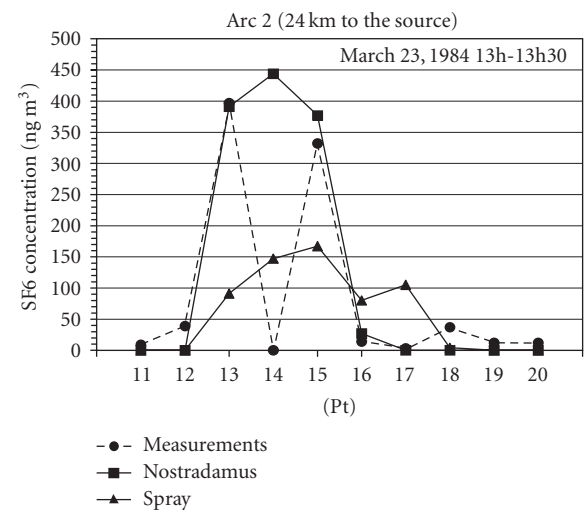

(b)

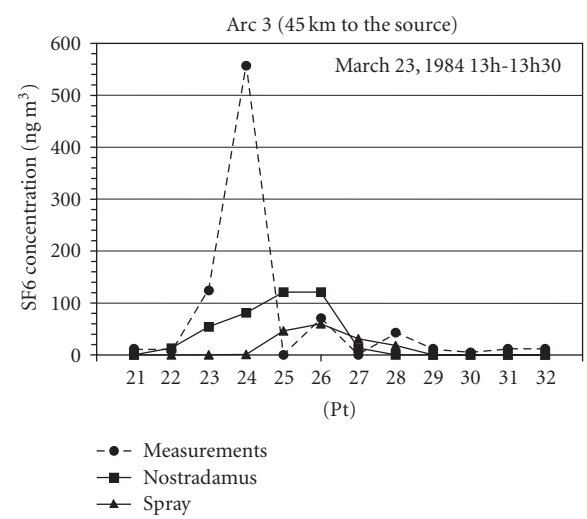

(c)

Figure 4: Comparison of SF6 concentration during experiment 2 on three arcs of monitoring points between measurements (at 1 meter above ground level) and NOSTRADAMUS and SPRAY calculations (at 10 meters above ground level).

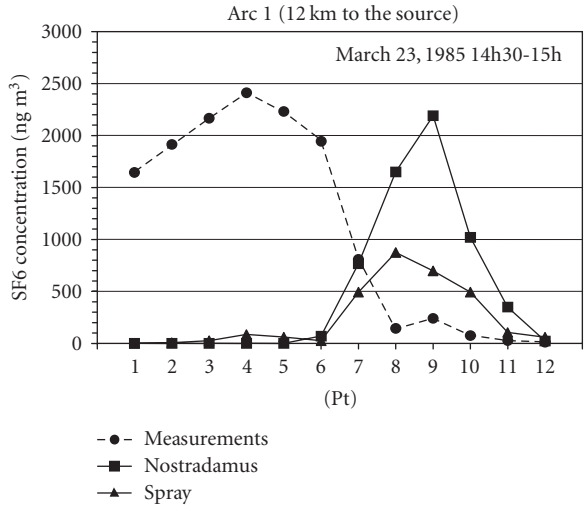

(a)

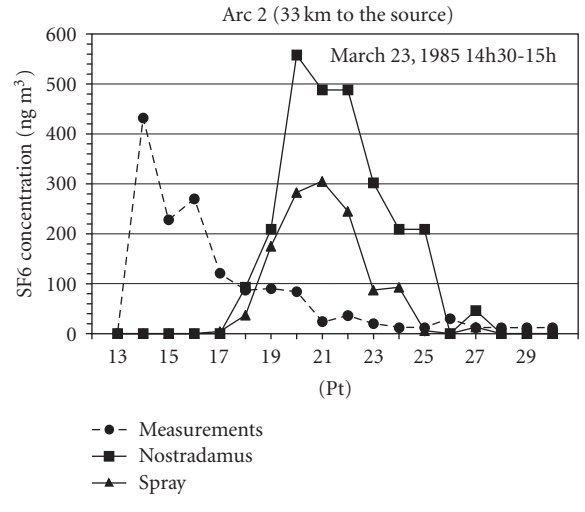

(b)

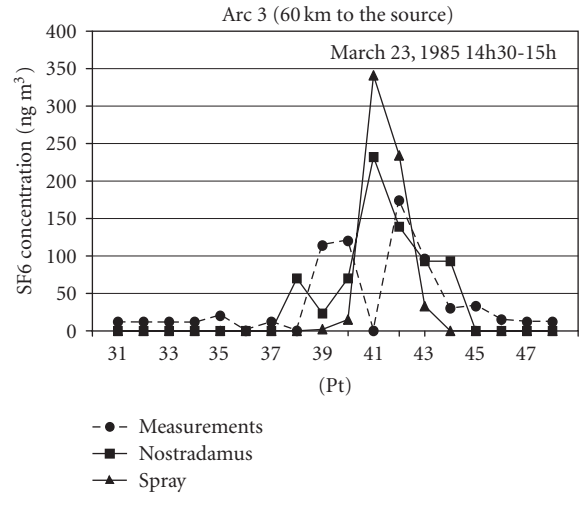

(c)

Figure 5: Comparison of SF6 concentration during experiment 3 on three arcs of monitoring points between measurements (at 1 meter above ground level) and NOSTRADAMUS and SPRAY calculations (at 10 meters above ground level).

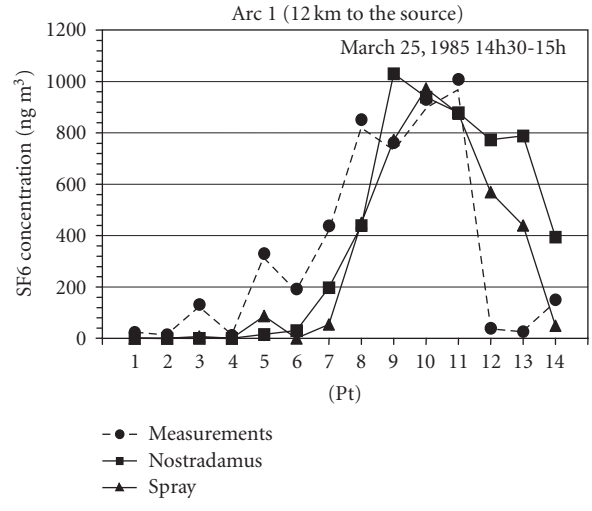

(a)

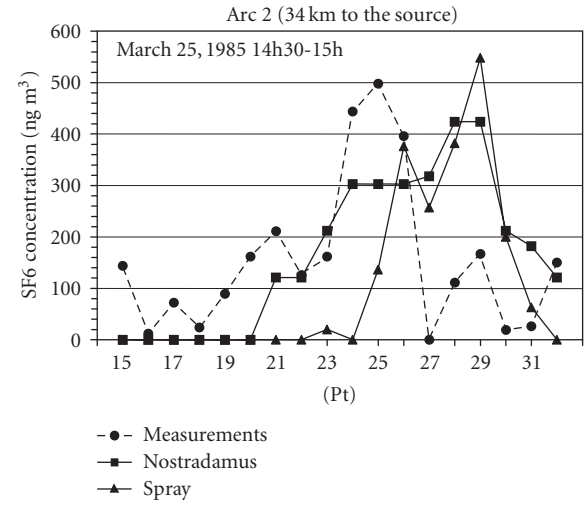

(b)

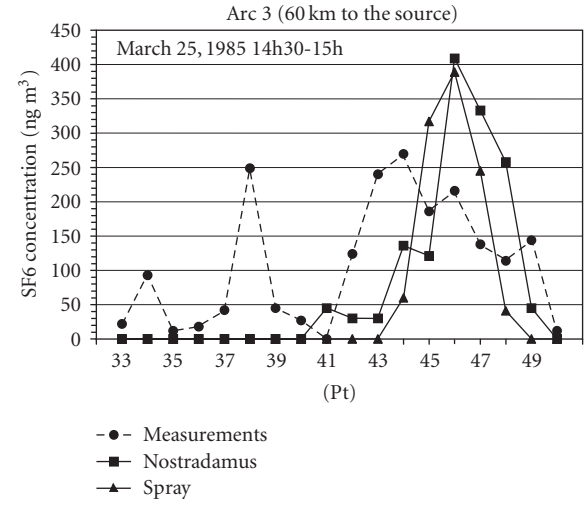

(c)

Figure 6: Comparison of SF6 concentration during experiment 4 on three arcs of monitoring points between measurements (at 1 meter above ground level) and NOSTRADAMUS and SPRAY calculations (at 10 meters above ground level).

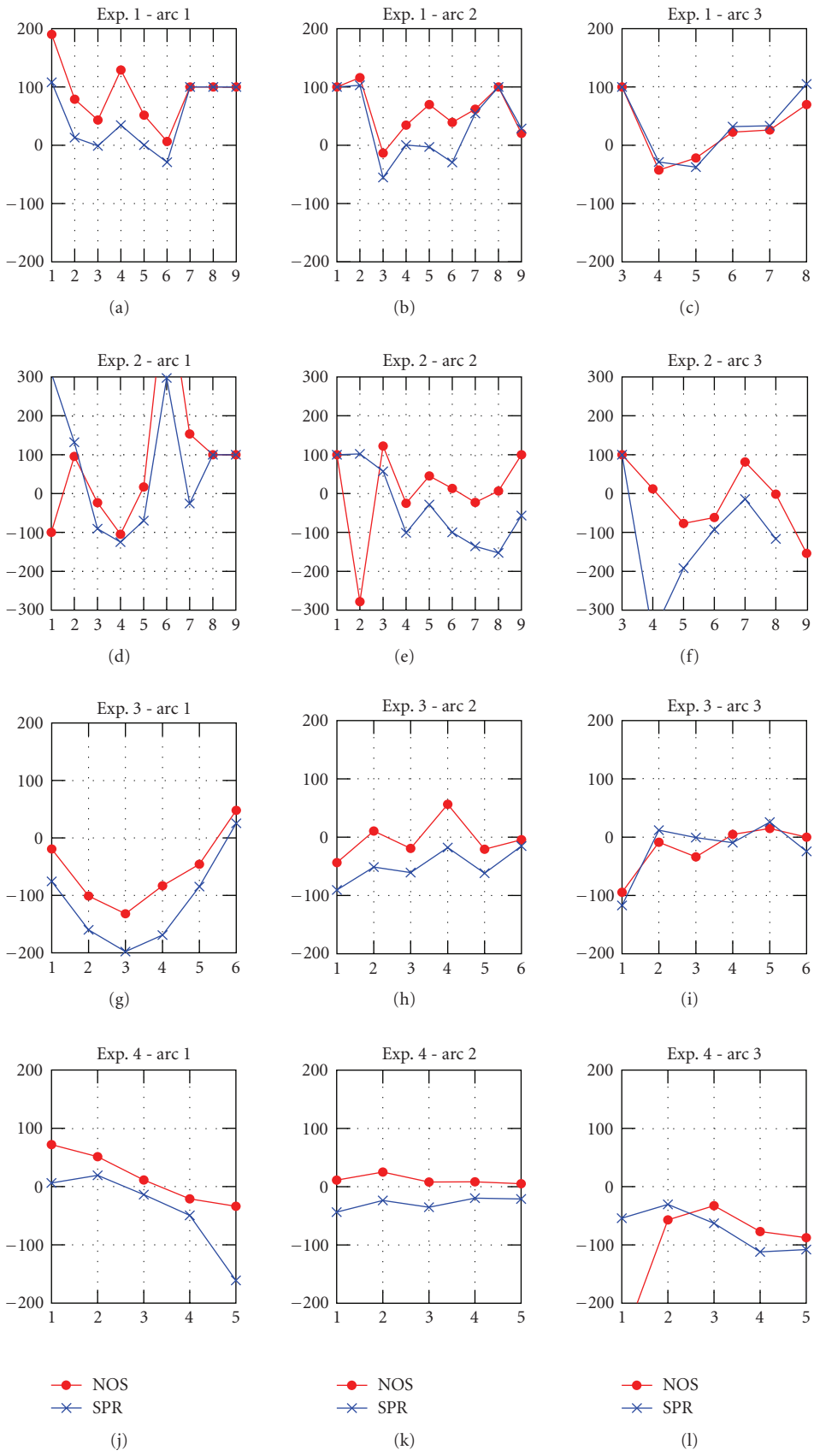

Figure 7: Normalized biases (expressed as a percentage) according to the experiment, of the arc of measurement points and time (NOS = Nostradamus code; SPR = MINERVE-SPRAY code).

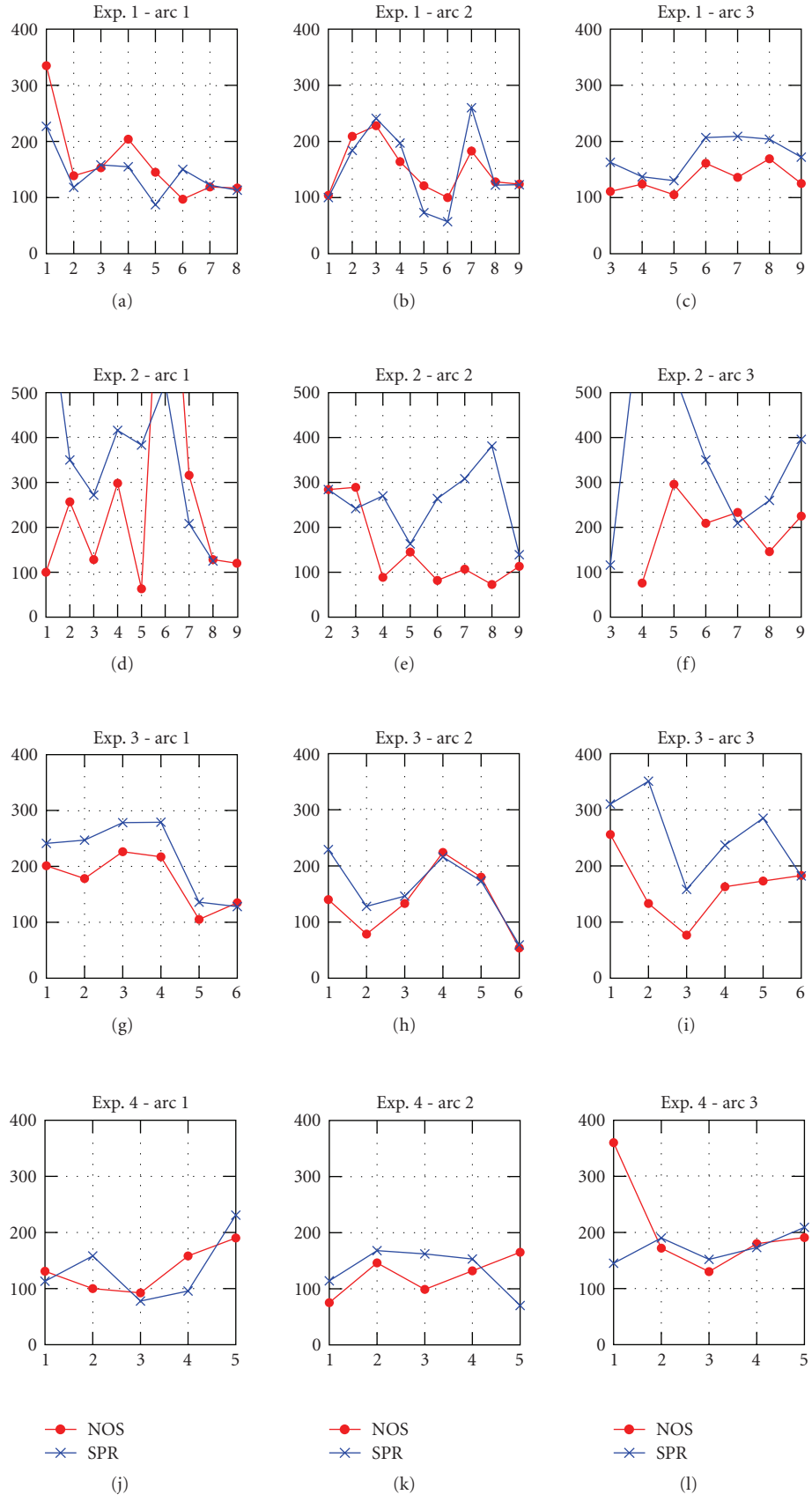

FIGURE 8: Normalized root mean square errors (expressed as a percentage) according to the experiment, of the arc of measurement points and time (NOS = NOSTRADAMUS code; SPR = MINERVE-SPRAY code).

concentrations, and statistical criteria would be misleading. Thirdly, we average the observations along the time, and we compare time averages at fixed spatial location (see Table 6). This temporal averaging is interesting to reveal some temporal shifts in the concentration peaks.

In Tables 4, 5, and 6, we can see that the data are not homogeneous because the total analysis and the analysis by experiment give different results in terms of normalized bias (NB), geometric mean bias (MG), normalized root mean square error (NRMS), geometric variance (VG), and fraction of data satisfying $0.5 < X/Y < 2$ (FAC2). From the NB values of Table 4, we note that SPRAY is more biased than NOSTRADAMUS, but their dispersion errors (NRMS) are equivalent. Moreover, we see that FAC2(Spray) < FAC2(Nostradamus) for all experiments. We conclude that the large biases of SPRAY are certainly due to several large errors. This is confirmed by the analysis of MG: except for experiment 1, MG values are smaller than 0.4 for NOSTRADAMUS, while MG values are closed to 0.6 for SPRAY. Indeed, MG is based on a logarithmic scale and provides a more balanced treatment of extreme high values.

By comparing NB, MG, NRMS, VG, and FAC2 of SPRAY and NOSTRADAMUS in Tables 4, 5, and 6, we can note that the worst results (large NB, small MG, large NRMS, large VG, and small FAC2) are in Table 4. We easily understand that the pairing of concentrations in time and space is the most stringent condition; and this explains the poor results in Table 4. Otherwise, we note that results in Table 5 are better than results in Table 6: the averaging in space gives better results than the averaging in time. This means that the two codes are more suited to reproduce the temporal scale than the spatial scale. The particles propagation velocities are relatively correct while errors on particles propagation angles induce stronger errors on calculated concentrations at specific locations.

Finally, to compare NOSTRADAMUS and SPRAY results, we carry out a finer graphical analysis by distinguishing the experiments, the arcs, and the time defined by different times (Figures 7 and 8). With the exception of experiment 2 where NB and NRMS are particularly high, the results according to the times are fairly consistent (i.e., of the same order of magnitude). According to the arc, the results are a little more variable. For the normalized bias, we can however note that the results of SPRAY for experiment 1 are better than those of NOSTRADAMUS, and vice versa for experiment 3. For the normalized standard error NRMS, the results obtained with SPRAY and NOSTRADAMUS are similar.

6. CONCLUSIONS

For the four experiments, we note a fairly good agreement between the results of MINERVE-SPRAY and NOSTRADAMUS, and to a lesser extent, with the field measurements. Because of the similarity of the models used in the two codes (based on the Lagrangian dispersion approach), and despite the fact that topography is used in MINERVE-SPRAY but not in NOSTRADAMUS, the results obtained with the two codes do not present notable differences.

The correlation is particularly good for experiment 1 (see Table 5 where FAC2 (Exp 1) > 0.5) during which the meteorological conditions remained nearly unchanged. This correlation is generally better for the sampling points located at an average distance of ten kilometers from the source (first arc of sampling points). For the points located far away (30, 45, and 60 kilometer of the source), some discrepancies appear between the model results and the measurements. This is probably due to the fact that, for these four experiments, only one weather station (near to the point source) was used for a domain surface area of 10 000 km^2, generating a uniform wind field over the whole calculation zone for both codes.

Another difference between calculations with MINERVE-SPRAY and field measurements is that the concentrations were measured at 1 meter above the ground in the field and the concentrations are calculated at 10 meters for the codes. This constitutes a major limitation for the codes, in particular for calculations when the number of input meteorological data is small. This applies in the majority of cases, particularly for nuclear accidents.

However, the order of magnitude of the concentrations found on the ground is predicted with the two dispersion codes used. The geographical situation (a valley bottom without topographic relief) and the relatively constant conditions of wind with time (wind of valley) supported the weak variations of the code results in spite of the use of only one weather station. Under conditions much more unfavorable, the results could have been much more dubious, in particular in the presence of accentuated topography or strongly turbulent weather conditions. We can however conclude that the 3D codes of Lagrangian dispersion can be used to estimate the transport of gaseous species in the atmosphere but, as in any use of complex models, it is important to have sufficient data points for a given experiment, in particular for complex scenarios where the need for several weather stations appears essential.

ACKNOWLEDGMENT

This work has been partly supported by the MRIMP project of the "Risk Control Domain" (CEA/Nuclear Energy Division/Nuclear Development and Innovation Division).

REFERENCES

[1] G. Brusasca, G. Tinarelli, and D. Anfossi, "Particle model simulation of diffusion in low wind speed stable conditions," *Atmospheric Environment. Part A*, vol. 26, no. 4, pp. 707–723, 1992.

[2] G. Tinarelli, *SPRAY 3.0—General description and user's guide*, 2001, ARIANET report.

[3] S. Galmarini, R. Bianconi, R. Bellasio, and G. Graziani, "Forecasting the consequences of accidental releases of radionuclides in the atmosphere from ensemble dispersion modelling," *Journal of Environmental Radioactivity*, vol. 57, no. 3, pp. 203–219, 2001.

[4] I. Lagzi, D. Karman, T. Turányi, A. S. Tomlin, and L. Haszpra, "Simulation of the dispersion of nuclear contamination using an adaptive Eulerian grid model," *Journal of Environmental Radioactivity*, vol. 75, no. 1, pp. 59–82, 2004.

[5] J. C. Chang and S. R. Hanna, "Air quality model performance evaluation," *Meteorology and Atmospheric Physics*, vol. 87, no. 1–3, pp. 167–196, 2004.

[6] P. Thomas, S. Vogt, and P. Gaglione, "Mesoscale atmospheric experiment using tracer and tetroons simultaneously," at Kernforschungszentrum/Karlsuhe. KfK 4147 EUR 10907 EN, p. 112, 1987.

[7] O. Oldrini, "Notice d'utilisation du code MINERVE 7.0," Rapport rt ARIA/2002.078, juillet 2002.

[8] G. Tinarelli, U. Giostra, E. Ferrero, et al., "SPRAY, a 3-D particle model for complex terrain dispersion," in *Proceedings of the 10th Symposium on Turbulence and Diffusion, American Meteorological Society*, pp. 147–150, Portland, Ore, USA, September-October 1992.

[9] G. Tinarelli, D. Anfossi, M. Bider, E. Ferrero, and S. Trini Castelli, "A new high performance version of the Lagrangian particle dispersion model SPRAY, some case studies," in *Proceedings of the 23rd CCMS-NATO Meeting*, pp. 499–507, Kluwer Academic Publishers, Varna, Bulgaria, September-October 1998.

[10] D. J. Thomson, "Random walk modeling of diffusion in inhomogeneous turbulence," *Quarterly Journal of the Royal Meteorological Society*, vol. 110, no. 466, pp. 1107–1120, 1984.

[11] D. J. Thomson, "Criteria for the selection of stochastic models of particle trajectories in turbulent flows," *Journal of Fluid Mechanics*, vol. 180, pp. 529–556, 1987.

[12] N. L. Byzova, V. A. Shnaidman, and V. N. Bondarenko, "Estimation of vertical wind profile in atmosphere boundary layer using ground-level data," *Meteorologia i Hydrologia*, vol. 11, pp. 75–83, 1987 (Russian).

[13] Y. S. Sedunov, Ed., *Atmosphere Handbook*, Gidrometeoizdat, Leningrad, Russia, 1991.

[14] RODOS, "Decision support system for off-site nuclear emergency management in Europe," Final Project Report RUR 19144 EN, European Commission, London, UK, 2000.

[15] V. V. Belikov, V. M. Goloviznin, V. Semenov, O. Sorokovikova, L. P. Starodubtseva, and A. Fokin, " Model of convective plume rise in the case of explosive energy release," *Izvestiya Akademii Nauk. Energetika*, vol. 4, pp. 100–117, 2000 (Russian).

[16] S. R. Hanna, G. A. Briggs, and R. P. Hosker, "Handbook on atmospheric diffusion," Report DOE/TIC-11223, p. 91, Department of Energy, Technical Information Center, Oak Ridge, Tenn, USA, 1982.

[17] D. G. Fox, "Judging air quality model performance: a summary of the AMS workshop on dispersion model performance," *Bulletin of the American Meteorological Society*, vol. 62, no. 5, pp. 599–609, 1981.

[18] C. J. Willmott, "Some comments on the evaluation of model performance," *Bulletin of the American Meteorological Society*, vol. 63, no. 11, pp. 1309–1313, 1982.

AUTHOR CONTACT INFORMATION

François Van Dorpe: CEA Cadarache, D2S/SPR, 13108 Saint Paul lez Durance Cedex, France; francois.vandorpe@cea.fr

Bertrand Iooss: CEA Cadarache, DEN/DER/SESI/LCFR, 13108 Saint Paul lez Durance Cedex, France; bertrand.iooss@cea.fr

Vladimir Semenov: Nuclear Safety Institute of Russian Academy of Sciences, 52 B. Tuskaya Street, Moscow 113191, Russia; sem@ibrae.ac.ru

Olga Sorokovikova: Nuclear Safety Institute of Russian Academy of Sciences, 52 B. Tuskaya Street, Moscow 113191, Russia; olga_sorokov@mail.ru

Alexey Fokin: Nuclear Safety Institute of Russian Academy of Sciences, 52 B. Tuskaya Street, Moscow 113191, Russia; fokin@ibrae.ac.ru

Yves Margerit: CEA Cadarache, DEN/DTN/SMTM/LMTE, 13108 Saint Paul lez Durance Cedex, France; yves.margerit@cea.fr